THE JOURNAL OF PHYSICAL CHEMISTRY A

ARTICLE

pubs.acs.org/JPCA

ReaxFF-*lg*: Correction of the ReaxFF Reactive Force Field for London Dispersion, with Applications to the Equations of State for Energetic Materials

Lianchi Liu,[†,‡] Yi Liu,[‡] Sergey V. Zybin,[‡] Huai Sun,[†] and William A. Goddard, III*[,‡]

[†]School of Chemistry and Chemical Engineering, Shanghai Jiao Tong University, Shanghai 200240, China

[‡]Materials and Process Simulation Center, 139-74, California Institute of Technology, Pasadena, California 91125, United States

Supporting Information

ABSTRACT: The practical levels of density functional theory (DFT) for solids (LDA, PBE, PW91, B3LYP) are well-known not to account adequately for the London dispersion (van der Waals attraction) so important in molecular solids, leading to equilibrium volumes for molecular crystals ~10−15% too high. The ReaxFF reactive force field is based on fitting such DFT calculations and suffers from the same problem. In the paper we extend ReaxFF by adding a London dispersion term with a form such that it has low gradients (*lg*) at valence distances leaving the already optimized valence interactions intact but behaves as $1/R^6$ for large distances. We derive here these *lg* corrections to ReaxFF based on the experimental crystal structure data for graphite, polyethylene (PE), carbon dioxide, and nitrogen and for energetic materials: hexahydro-1,3,5-trinitro-1,3,5-*s*-triazine (RDX), pentaerythritol tetranitrate (PETN), 1,3,5-triamino-2,4,6-trinitrobenzene (TATB), and nitromethane (NM). After this dispersion correction the average error of predicted equilibrium volumes decreases from 18.5 to 4.2% for the above systems. We find that the calculated crystal structures and equation of state with ReaxFF-*lg* are in good agreement with experimental results. In particular, we examined the phase transition between α-RDX and γ-RDX, finding that ReaxFF-*lg* leads to excellent agreement for both the pressure and volume of this transition occurring at ~4.8 GPa and ~2.18 g/cm^3 density from ReaxFF-*lg* vs 3.9 GPa and ~2.21 g/cm^3 from experiment. We expect ReaxFF-*lg* to improve the descriptions of the phase diagrams for other energetic materials.

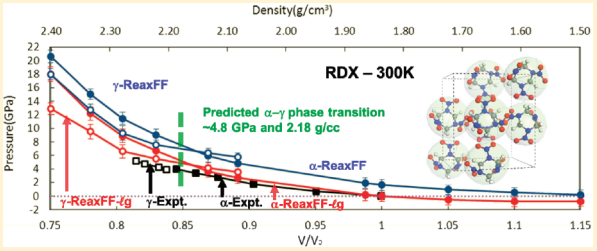

1. INTRODUCTION

The ReaxFF reactive force field method[1] has been applied successfully in a variety of reactive dynamics (RD) simulations of hydrocarbon organic compounds,[2] polymers,[3] energetic materials,[4−9] metal oxides,[10−13] and transition metal catalysts,[14] studying rapid reaction processes including pyrolysis,[15] explosions,[6,7] shock processes,[5,8,16] and combustion.[2,15] Thus ReaxFF has enabled the study of chemical reactions in large condensed phase systems (up to millions of atoms) at large time scales (up to 100 ns), providing mechanistic and conceptual information not readily available from experiments or quantum mechanics (QM).

Particularly important applications of ReaxFF have been to energetic materials, which involve a complex sequence of reactions and multiple intermediates, many of which are difficult to detect, making it difficult to extract a mechanistic understanding. Thus, ReaxFF reactive dynamics (ReaxFF-RD) has been used successfully to study shock transformation for many energetic materials including hexahydro-1,3,5-trinitro-1,3,5-*s*-triazine (RDX),[5,7,8] pentaerythritol tetranitrate (PETN),[16] octahydro-1,3,5,7-tetranitro-1,3,5,7-tetrazocine (HMX),[6] 1,3,5-triamino-2,4,6-trinitrobenzene (TATB),[6] triacetonetriperoxide (TATP),[4] and nitromethane (NM).[9] Here ReaxFF-RD calculations were used to study the decomposition mechanisms and shock behaviors of these materials, with results in good agreement with experiment and QM, validating the accuracy of ReaxFF for studying the reaction mechanisms.

The philosophy in developing the ReaxFF reactive force field was to use only data from consistent quantum mechanics (QM) calculations (generally the B3LYP flavor of DFT with the 6-31G** basis set). This created a problem for solids since the practical levels of DFT for solids (LDA, PBE, PW91, B3LYP) are well-known not to account adequately for the London dispersion (van der Waals (vdW) attraction) so important in molecular solids, leading to equilibrium volumes ~10−15% too high. Thus our previous ReaxFF studies also did not include sufficient London dispersion. The result is that ReaxFF and DFT calculations on energetic materials both lead to equilibrium densities ~10−15% larger than experiment.[6,7,16]

In fact, ReaxFF includes a vdW term, using a Morse function that is repulsive for short R (Pauli repulsion) and attractive for large R (van der Waals attraction). However since no data were included to train these vdW terms to fit the long-range London dispersion, they rather play a role in modulating the various valence

Received: February 17, 2011
Revised: August 22, 2011
Published: September 02, 2011

interactions by including the Pauli repulsion or steric interactions so important for valence structures.

Since we do not want to modify the parts of ReaxFF that already account for these valence interactions, but we now want to improve the long-range dispersion to obtain the correct density for molecular crystals, we introduce into ReaxFF an additional vdW-like interaction, chosen to have a form that has little effect at the distances relevant to valence interactions while accounting for long-range London dispersion. To accomplish this, we use the same low-gradient (*lg*) form proposed by Liu and Goddard for improving the description of London dispersion in standard DFT methods,[17] leading to the ReaxFF-*lg* force field.

In this work, we report dispersion corrections for ReaxFF, based on this low-gradient model (ReaxFF-*lg*), for the energetic materials RDX, PETN, TATB, and NM plus graphite, polyethylene, solid carbon dioxide, and solid N_2, using the low temperature crystal structures to determine the *lg* correction parameters. Here we consider densities and heats of sublimation of these materials in the training sets. Then the fitted parameters are extended to energetic materials and refined to obtain the final parameters. To validate the ReaxFF-*lg* method, we calculated the equations of state of these materials and compared the results with results from experiments at room temperature.

2. METHOD AND COMPUTATIONAL DETAILS

In ReaxFF-*lg*, the total energy of the system can be expressed as

$$E_{\text{Reax-}lg} = E_{\text{Reax}} + E_{lg} \tag{2.1}$$

where E_{Reax} is the energy evaluated from the previous ReaxFF force field:

$$\begin{aligned} E_{\text{Reax}} = {} & E_{\text{bond}} + E_{\text{lp}} + E_{\text{over}} + E_{\text{under}} + E_{\text{val}} \\ & + E_{\text{pen}} + E_{\text{coa}} + E_{\text{tors}} + E_{\text{conj}} \\ & + E_{\text{H-bond}} + E_{\text{vdW}} + E_{\text{Coulomb}} \end{aligned} \tag{2.2}$$

and E_{lg} is the long-range-correction terms using the low-gradient model:

$$E_{lg} = -\sum_{ij,\, i<j}^{N} \frac{C_{lg,\,ij}}{r_{ij}^{\,6} + dR_{eij}^{\,6}} \tag{2.3}$$

Here r_{ij} is the distance between atom i and atom j, R_{eij} is the equilibrium vdW distance between atoms i and j, and $C_{lg,ij}$ is the dispersion energy correction parameter. For each atomic pair ij, we use the geometric combination rules for both R_{eij} and $C_{lg,ij}$, unless the off-diagonal parameters are listed specifically for a particular pair. Here d is a scaling factor, but we set $d = 1.0$ since we found no need for scaling in this work. R_e is taken as the vdW radii in the Universal force field (UFF)[18] (convenient since these values are defined in UFF up to element 103, Lr), as shown in Table 1, and only the C_{lg} parameters are fitted.

Low temperature crystal structures of graphite ($P6_3mc$),[19] polyethylene (PE, *Pnam*),[20] carbon dioxide ($Pa3$),[21] and solid nitrogen[22] ($Pa3$) were selected to determine the dispersion correction parameters for ordinary organic materials. Graphite and polyethylene are prototypes for determining the dispersion corrections for C−C, C−H, H−H and were used previously for studying or testing the vdW interactions.[23,24] Carbon dioxide and solid nitrogen are molecular crystals suitable for determining the dispersion corrections for C−O, O−O, and N−N. On the basis of these parameters fitted from these ordinary organic materials,

Table 1. ReaxFF-*lg* Dispersion Correction Parameters[a]

	R_e (Å)		C_{lg} (kcal/mol·A^6)
C	1.9255	C−C	0
N	1.8300	H−C	0
O	1.7500	O−O	624
H	1.4430	N−N	1239
		C−H	0
		H−O	0
		H−N	295
		C−O	632
		C−N	650
		O−N	880

[a] See eq 2.3 for definitions.

Chart 1. Procedure for Fitting Dispersion Correction Parameters

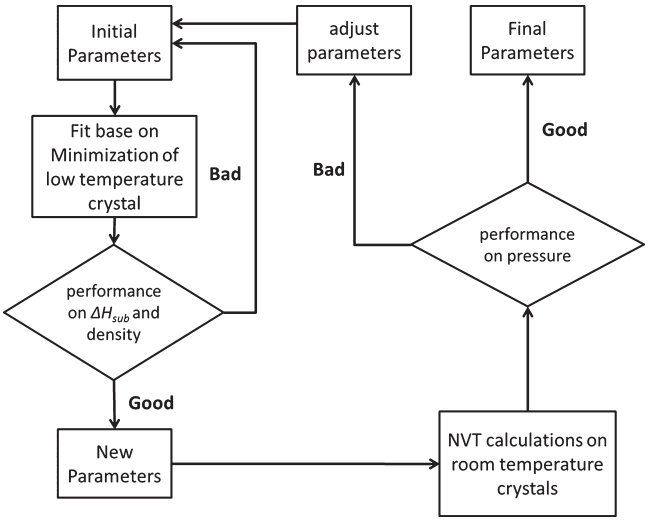

we proceeded to determine the C−N, N−O, H−N, and H−O correction parameters for energetic materials.

The ReaxFF force field used for our fitting is based on the force field of energetic materials in ref 7. The final full set of parameters is in the Supporting Information. In the fitting procedure (Chart 1), the density and heat of sublimation at low temperature were first used to obtain initial *lg* parameters. Then these parameters were used to describe the pressure in NVT calculations at room temperature with the experimental density. The parameters were adjusted to reduce the calculated error in the pressure, until the error was ±0.5 GPa. We then started with these modified parameters as initial parameters for the next round fitting to the low temperature crystal densities and heats of sublimation. The goal was to find parameters providing a good description for both low temperature and room temperature.

To validate the ReaxFF-*lg* force field, we calculated the equation of state (EOS) at room temperature for multiple unit cells of 4 × 4 × 2 hexagonal graphite, 2 × 3 × 6 polyethylene, 3 × 3 × 3 carbon dioxide, 2 × 2 × 2 RDX, 3 × 3 × 3 PETN, 3 × 3 × 3 TATB, and 3 × 3 × 3 NM.

Initial cells at each volume were built by scaling the center of mass of each molecule in the cell and minimizing using the conjugate gradients method. For each system, the ReaxFF-*lg* molecular

Table 2. Heats of Sublimation and Cell Parameters from Experiment, ReaxFF, and ReaxFF-*lg*

	heat of sublimation[a] (kcal/mol)			cell parameters				density (error %)	
	expt	ReaxFF-*lg*	ReaxFF		expt	ReaxFF-*lg*	ReaxFF	ReaxFF-*lg*	ReaxFF
graphite	1.19[c]	1.81	1.81	*a*	2.462	2.513	2.513	−6.34	−6.34
				c	6.656	6.601	6.601		
PE	1.838[d]	2.20	2.20	*a*	7.121	7.051	7.051	4.94	4.94
				b	4.851	4.648	4.648		
				c	2.548	2.553	2.553		
CO_2	6.44[e]	5.72	1.46	*a*	5.540	5.700	6.302	−8.92	−47.2
N_2	1.65[f]	4.84	0.68	*a*	5.644	5.667	6.152	−1.23	−29.51
RDX	32.1[g]	31.15	17.41	*a*	12.938[b]	12.960	13.357	−0.82	−28.45
				b	11.331[b]	11.378	11.960		
				c	10.502[b]	10.527	12.379		
PETN	37.62[h]	55.55	30.43	*a*	9.252[b]	9.098	9.542	−0.89	−16.88
	55.7[i]			*c*	6.579[b]	6.864	7.229		
TATB	40.21[j]	37.72	23.67	*a*	9.010	9.150	9.393	4.09	−6.30
				b	9.028	8.960	9.041		
				c	6.608	6.288	6.728		
NM	11.30[k]	16.92	10.29	*a*	5.183	4.926	5.062	6.69	−8.04
				b	6.236	6.537	7.128		
				c	8.518	7.978	8.244		

[a] Calculated at experimental temperature. [b] Extrapolated from room temperature experimental data. [c] From ref 39. [d] From ref 40. [e] From ref 41 (from 195 to 217 K). [f] From ref 42 (from 0 to 77.3 K). [g] From ref 43 (from 343 to 447 K). [h] From ref 44 (from 356 to 382 K). [i] From ref 45 (from 352 to 423 K). [j] From ref 46 (from 403 to 450 K). [k] Estimated value from ref 47.

dynamics simulations used the NVT ensemble (T = 300 K) with 0.1 fs time step. We equilibrated for 5 ps followed by 5 ps for property analysis. These calculations use the Berendsen thermostat with 10 fs damping constant. The long-range interactions, including vdW(+*lg*) and Coulomb interactions are calculated using a 10 Å cutoff combined with the taper function (seventh order spline) using R_{on} = 0 and $R_{off} = R_{cut}$. For cases in which the minimum box side length is less than 20 Å, we choose half the value of this minimum box side length as the cutoff. The charges for the Coulomb interactions are calculated using the electronegativity-equalization method (EEM).[25,26]

Particularly interesting is the case of RDX, where a phase transition is known to occur at high pressure. Here we used both α-RDX and γ-RDX crystal structures to calculate the EOS and investigate the phase transition.

We then investigated the effect of the *lg* dispersion correction on the performance of ReaxFF for describing thermal decomposition reactions of RDX, PETN, TATB, and NM, where the training set includes 1441 reactions. These reactions are from the previous training sets of ReaxFF on energetic materials containing the bond stretching and breaking, angle and torsion bending, and thermal decomposition reaction pathways for RDX, PETN, NM, TATB, TATP, and HMX systems. We compared the ReaxFF-*lg* results with the previous unmodified ReaxFF to ensure that introducing dispersion does not affect the description of chemical reactions.

3. RESULTS AND DISCUSSION

3.1. Fitting Results and Unit Cell Performance. The final ReaxFF-*lg* parameters are listed in Table 1. Table 2 shows the heats of sublimation and cell parameters predicted from both ReaxFF and ReaxFF-*lg* and compares the values with values from experiment. In Table 2, the heats of sublimation are calculated at the experimental temperature for each case and the cell parameters are compared at low temperature (0 K). We see that the cell parameters from ReaxFF-*lg* are in good agreement with experiment. The errors in densities are listed in Table 2, which shows that ReaxFF-*lg* is significantly improved compared with ReaxFF. The heats of sublimation calculated by ReaxFF-*lg* are in good agreement with experiment. Thus Table 2 shows that ReaxFF-*lg* reduces the relative errors in ΔH_{sub} to −3.0, −0.3, and −6.2%, compared with −45.8, −45.4, and −41.1%, respectively, from previous ReaxFF.

Figure 1 compares the structures of the optimized ReaxFF-*lg* unit cells with the experimental structures at low temperatures (in yellow), superimposed to have the centers of masses coincide. The experimental structures at low temperature were used to extrapolate to the cell at 0 K, as shown in Table 2. We calculated the root-mean-square deviations (rmsd's) of the atomic displacements based on these center-of-mass superimposed structures. The rmsd values for RDX, PETN, TATB, and NM are 3.62, 1.64, 1.17, and 0.87 Å, respectively. We found excellent agreement for the four energetic materials studied here, indicating that the ReaxFF-*lg* predicts crystal structures reasonably well.

Figure 2 shows the radial distribution functions for the molecular centers of mass at room temperature from ReaxFF-*lg*, compared with experiments and ReaxFF. These peaks show the distributions of the distances of molecular pairs in the crystals. We see that ReaxFF-*lg* is much closer to experiment than ReaxFF. For RDX and PETN, ReaxFF-*lg* predicts the same position of each molecule in the crystal cell as in the experiments. In the cases of NM and TATB, there are some differences in the peak positions of ReaxFF-*lg* compared with experiments, but they are much improved compared with ReaxFF.

In the case of TATB, the first peak (∼5.0 Å) refers to the closest molecular pairs between layers and the second peak (6.0−8.0 Å)

refers to the second short distance molecule pairs between layers, while the third peak (9.0 Å) refers to the neighboring pairs in the same layer. The inconsistency between the second peaks between ReaxFF, ReaxFF-*lg*, and experiment arises because ReaxFF-*lg* predicts a shorter layer distance (2.95 Å) than experiment (3.14 Å), while ReaxFF gives a slightly longer value (3.15 Å).

In the case of NM, the first peak refers to the neighboring pairs in the crystal; the difference between ReaxFF, ReaxFF-*lg*, and experiment arises from overestimating the density of ReaxFF-*lg* by 7% while ReaxFF underestimates the density by −8%.

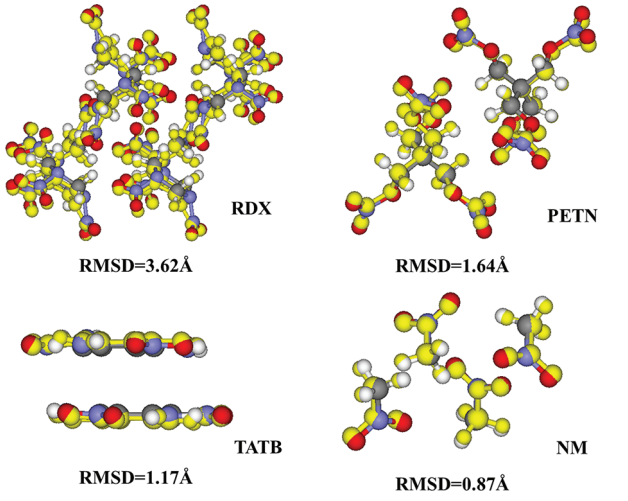

Figure 1. Comparisons of molecular structures in the crystal unit cell from ReaxFF-*lg* with experimental structures at low temperature (0 K). Yellow structures are the reference structures from experiments or extrapolation, and colored structures are the optimized structures from ReaxFF-*lg*.

3.2. Equation of State. To validate ReaxFF-*lg*, we first consider the equations of state (EOSs) for graphite,[27] polyethylene,[28] and solid carbon dioxide[29] at high pressure and room temperature as test cases. The comparisons of EOSs between experiments and ReaxFF(-*lg*) for graphite, polyethylene, and carbon dioxide at room temperature are presented in Figures 3, 4, and 5, respectively.

The predicted pressures for both graphite and polyethylene are slightly underestimated (by −5 and −14%) at each volume (Figures 3 and 4). Including dispersion interaction would further lower the pressures. Thus we do not include dispersion corrections for H−H, C−H, and C−C interactions.

In the case of solid carbon dioxide, ReaxFF-*lg* predicts pressures consistent with experiment at low compression, but underestimates

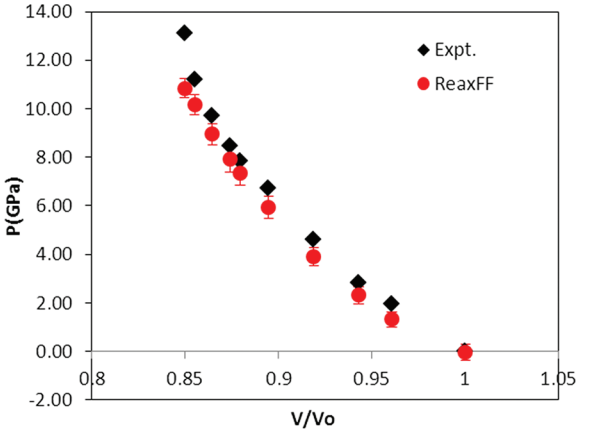

Figure 3. Equation of state of graphite at room temperature (300 K). The black diamonds are experimental results from Hanfland;[27] the red circles are ReaxFF-*lg* results, which are the same as for ReaxFF.

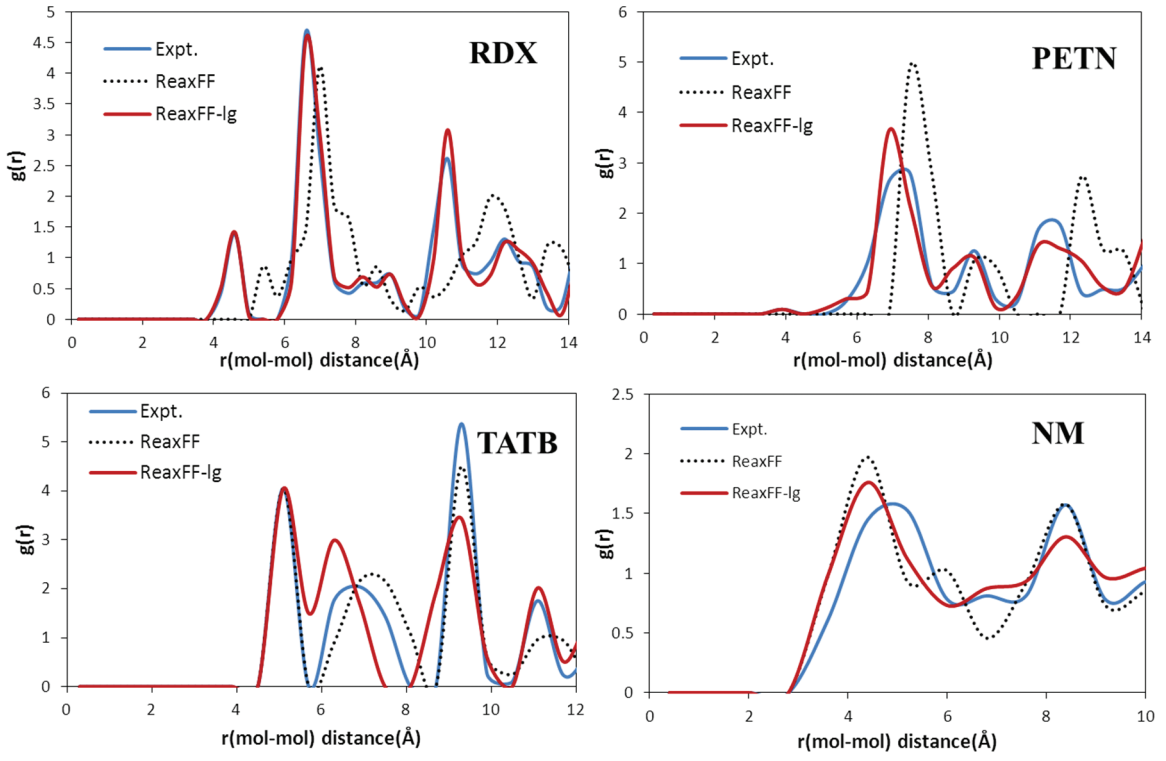

Figure 2. Comparisons of radial distribution functions for the center of mass of RDX, PETN, NM, and TATB at room temperature. Blue lines are experimental results, black dotted lines are ReaxFF results, and red lines are ReaxFF-*lg* results.

dx.doi.org/10.1021/jp201599t |*J. Phys. Chem. A* 2011, 115, 11016–11022

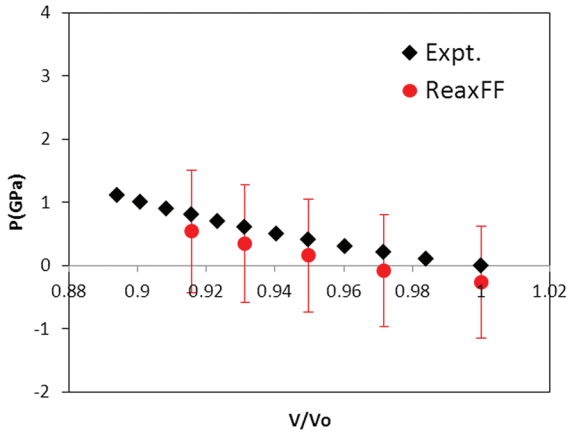

Figure 4. Equation of state of polyethylene at room temperature (300 K). Black diamonds are the experimental results from Ito,[28] while the red circles are ReaxFF-*lg* results, which are the same as ReaxFF.

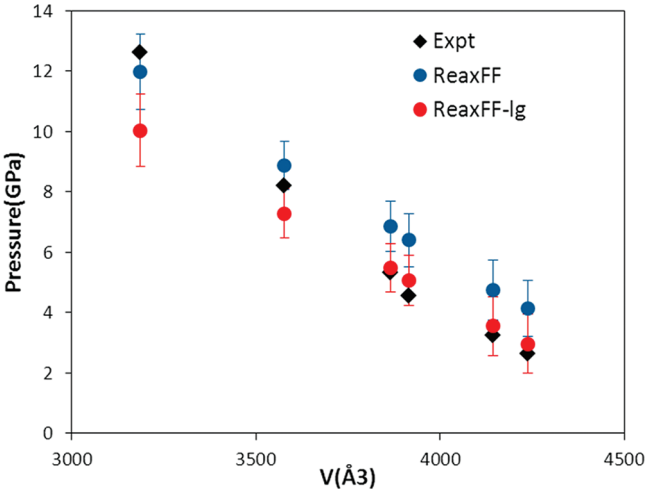

Figure 5. Equation of state of solid carbon dioxide at room temperature. The black diamonds are experimental results from Yoo,[29] the blue circles are ReaxFF, and the red circles are ReaxFF-*lg*. Note that ReaxFF does not find the phase transition at 7 GPa suggested by Aoki.[30]

the pressures at high compression. This may arise from inaccurate Coulomb interactions. For example, EEM[25] leads to charges of $q(C) = 0.7$ and $q(O) = -0.35$ for CO_2 compared with 0.5 and −0.25 from QM. We note here that ReaxFF does not find the phase transition at 8−12 GPa suggested by Aoki.[30] These results indicate that ReaxFF-*lg* leads to EOSs for ordinary organic materials at ambient temperature in reasonable agreement with experiment.

Using ReaxFF-*lg*, we predicted the equation of state of RDX at room temperature in Figure 6. We calculated the isotherms for the α-RDX and γ-RDX phases to investigate the phase transition between them at high pressure. Although several experimental papers have reported a range of results for the α-phase to γ-phase transition in RDX, Davidson[31] in 2008 established that this phase transition occurs at ∼2.21 g/cm^3 at 3.9 GPa. This agrees well with our results using ReaxFF-*lg* (∼2.15 g/cm^3 at ∼4.8 GPa) and those of Munday[32] (∼2.03 g/cm^3 at 2.1 GPa) using the Smith RDX force field.[33] ReaxFF also led to the phase transition at the same density, but at much higher pressure, ∼6.6 GPa.

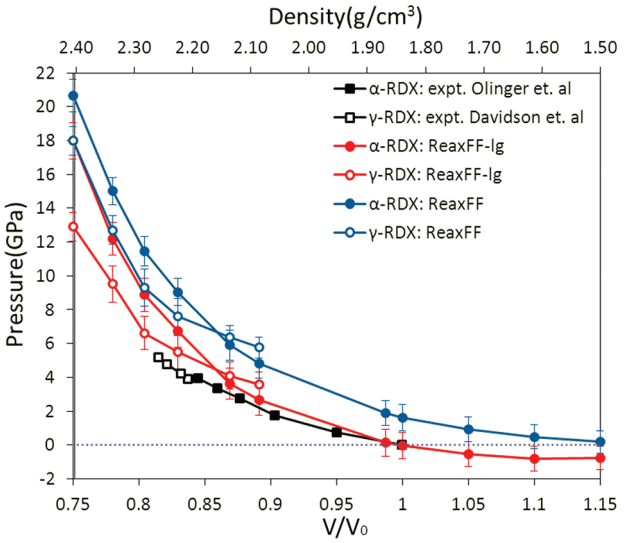

Figure 6. Equation of state of RDX at room temperature. The black filled squares are the experimental results from Olinger[48] for α-RDX; the open squares are experimental results from Davidson[31] for γ-RDX; the red filled and open circles are ReaxFF-*lg* results for α-RDX and γ-RDX, respectively; the blue filled and open circles are the ReaxFF results for α-RDX and γ-RDX, respectively. ReaxFF-*lg* predicts the α to γ phase transition to be at $\sim 0.85V/V_0$ (∼2.18 g/cm^3) and ∼4.8 GPa, in excellent agreement with experiment $\sim 0.83V/V_0$ (∼2.21 g/cm^3) and 3.9 GPa.

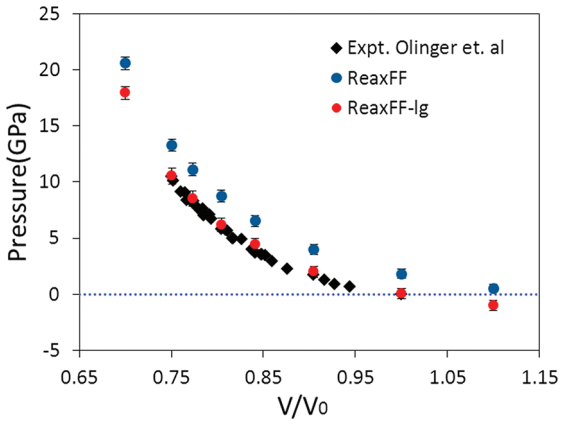

Figure 7. Equation of state of PETN at room temperature. Black diamonds are experimental results from Olinger,[34] blue circles are ReaxFF results, and red circles are ReaxFF-*lg* results. ReaxFF-*lg* leads to excellent agreement with experiment throughout the range of pressure.

The computed and experimental EOSs for PETN are compared in Figure 7. Here we see that ReaxFF-*lg* compares well with the experiments from Olinger et al,[34] whereas ReaxFF overestimates the pressure at high compression. ReaxFF-*lg* underestimates the pressure at low pressure but gives consistent results at high pressure.

In the case of TATB (Figure 8), ReaxFF-*lg* underestimates the pressure at low compression but agrees with experiment (Stevens[35]) at high compression. The inconsistency of TATB at low compression may come from overestimating the electrostatic interactions of TATB since neighboring NO_2 and NH_2 groups in the same layer lead to a large induced dipole, which induces strong Coulomb interactions between layers which might affect the compression.

dx.doi.org/10.1021/jp201599t |*J. Phys. Chem. A* 2011, 115, 11016–11022

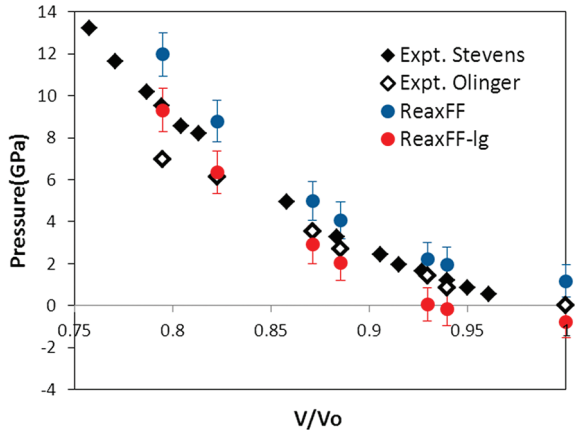

Figure 8. Equation of state of TATB at room temperature. The filled black diamonds are experimental results from Stevens,[35] and the open black diamonds are experimental results from Olinger.[49] The blue circles are previous ReaxFF results, while the red circles are the new ReaxFF-*lg* results.

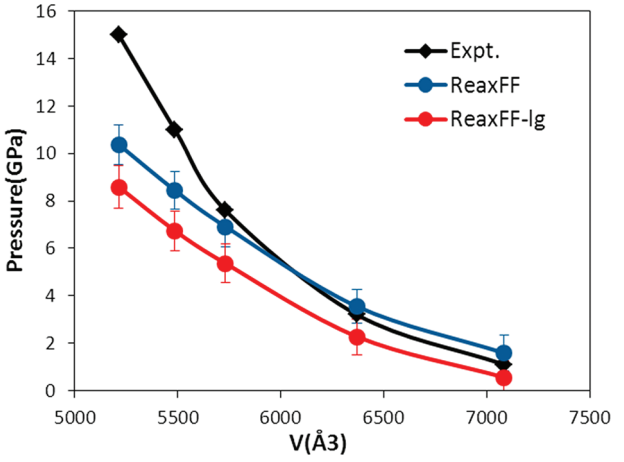

Figure 9. Equation of state of nitromethane at room temperature. Black diamonds are experimental results from Olinge,[34] blue circles are previous ReaxFF results, and red circles are new ReaxFF-*lg* results.

To test such effects, we plan additional optimization of ReaxFF for energetic materials where we use QEq[26] rather than EEM[25] charges and where we allow the charges to evolve with a damping constant rather than being adjusted every time step. It is also possible that the low pressure discrepancy results from the fixed ratios of cell parameters used in our NVT ensemble.

For NM (Figure 9), ReaxFF-*lg* agrees with experiment at low pressure, but underestimates the pressure at high compression. Phase transitions of solid nitromethane at ambient temperature have been reported at approximately 3, 7.5, 13.2, and 25 GPa,[36−38] where it is believed that they may be caused by rotations of the methyl groups. Our current studies did not attempt to locate these transitions accurately (which would require NPT calculations on larger cells and traversing both pressure and temperature from above and below the transitions). For >7.5 GPa we did find that structures with rotated methyl groups have energies similar to those of structures with unrotated methyl groups.

In these NVT-MD simulations, the pressure fluctuation is about ±1 GPa, which arises from the relatively small size of the

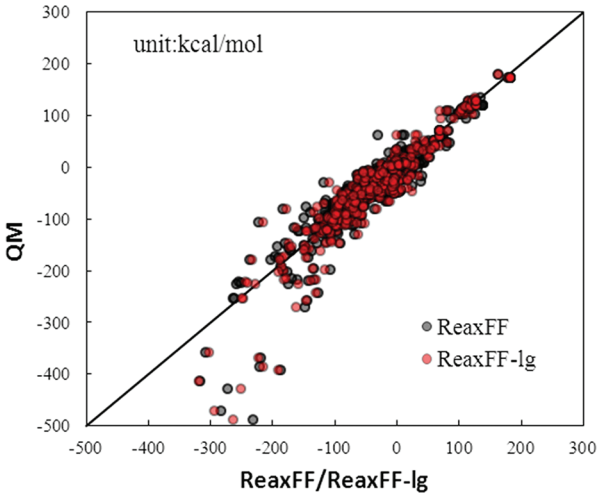

Figure 10. Comparison of reaction energies (kcal/mol) for ReaxFF (gray dots) and ReaxFF-*lg* (red dots) over the QM data set used to train ReaxFF.

simulation cells. These slight inconsistencies of the ReaxFF-*lg* for EOSs may indicate that the Coulomb interactions calculated from EEM are not sufficient for an accurate description of the hydrogen bonds, where polarization between nitro and amino groups may play a critical role in the intermolecular interactions.

Also, our use of the NVT ensemble introduces some uncertainties in the calculations of equations of state due to the fixed box sizes. A more rigorous approach is to generate the equations of state through isotherm−isostress (NST)-MD simulations. Before attempting this we plan to readjust the ReaxFF parameters with very careful attention to providing as accurate as possible the energies and barriers for the various molecular conformations in the different phases along with more accurate descriptions of long-range interactions. This will be the emphasis for a future study.

3.3. Reaction Performance. Figure 10 compares with QM the reaction energies of energetic materials calculated from ReaxFF and ReaxFF-*lg*. More detailed information is included in the Supporting Information. This shows that ReaxFF-*lg* leads to results consistent with ReaxFF for describing chemical reactions. Thus the *lg* dispersion corrections have little effect on the descriptions of chemical reactions.

4. CONCLUSIONS

We report the ReaxFF-*lg* dispersion corrections to ReaxFF, which improves intermolecular interactions for the energetic materials RDX, PETN, TATB, and NM. We used graphite, polyethylene, carbon dioxide, and nitrogen solids to determine correction parameters to reproduce the low temperature density and heat of sublimation. Then these ReaxFF-*lg* parameters were fitted and extended to energetic molecular crystals.

We see that ReaxFF-*lg* predicts equations of states consistent with experiment, making significant improvements of intermolecular interactions compared with original ReaxFF. Moreover, ReaxFF-*lg* predicts successfully the phase transition of RDX at high pressure. In addition, ReaxFF-*lg* leads to negligible effects on chemical reaction energies. Thus we recommend ReaxFF-*lg* for improving the intermolecular interactions in ReaxFF.

■ ASSOCIATED CONTENT

Supporting Information. Final full set of parameters and reaction energies of energetic materials calculated by ReaxFF-*lg* and ReaxFF. This material is available free of charge via the Internet at http://pubs.acs.org.

■ AUTHOR INFORMATION

Corresponding Author
*E-mail: wag@wag.caltech.edu.

■ ACKNOWLEDGMENT

Financial support from the National Science Foundation of China (No. 20473052), NSAF funding (No. 10676021), and the National Basic Research Program of China (Nos. 2003CB615804 and 2007CB209701) is gratefully acknowledged. We acknowledge the funding from the China Scholarship Council (No. 2009623057, Cliff Bedford). In addition, we acknowledge Funding ONR (N00014-09-1-0634), ARO-MURI (W911NF-08-1-0124, Ralph Anthenien), and ARL HPC (with help from Betsy Rice).

■ REFERENCES

(1) van Duin, A. C. T.; Dasgupta, S.; Lorant, F.; Goddard, W. A. *J. Phys. Chem. A* **2001**, *105*, 9396.
(2) Chenoweth, K.; van Duin, A. C. T.; Goddard, W. A. *J. Phys. Chem. A* **2008**, *112*, 1040.
(3) Chenoweth, K.; Cheung, S.; van Duin, A. C. T.; Goddard, W. A.; Kober, E. M. *J. Am. Chem. Soc.* **2005**, *127*, 7192.
(4) van Duin, A. C. T.; Zeiri, Y.; Dubnikova, F.; Kosloff, R.; Goddard, W. A. *J. Am. Chem. Soc.* **2005**, *127*, 11053.
(5) Nomura, K.-i.; Kalia, R. K.; Nakano, A.; Vashishta, P.; van Duin, A. C. T.; Goddard, W. A. *Phys. Rev. Lett.* **2007**, *99*, 148303.
(6) Zhang, L.; Zybin, S. V.; van Duin, A. C. T.; Dasgupta, S.; Goddard, W. A.; Kober, E. M. *J. Phys. Chem. A* **2009**, *113*, 10619.
(7) Strachan, A.; Kober, E. M.; van Duin, A. C. T.; Oxgaard, J.; Goddard, W. A., III. *J. Chem. Phys.* **2005**, *122*, 054502.
(8) Strachan, A.; van Duin, A. C. T.; Chakraborty, D.; Dasgupta, S.; Goddard, W. A. *Phys. Rev. Lett.* **2003**, *91*, 098301.
(9) Guo, F.; Zhang, H.; Cheng, X. *J. Theor. Comput. Chem.* **2010**, *9*, 315.
(10) Chenoweth, K.; Goddard, W., III. *Angew. Chem., Int. Ed.* **2009**, *48*, 7630.
(11) Goddard, W. A., III; Mueller, J. E.; Chenoweth, K.; van Duin, A. C. T. *Catal. Today* **2010**, *157*, 71.
(12) Goddard, W.; van Duin, A.; Chenoweth, K.; Cheng, M.; Pudar, S.; Oxgaard, J.; Merinov, B.; Jang, Y.; Persson, P. *Top. Catal.* **2006**, *38*, 93.
(13) Goddard, W.; Chenoweth, K.; Pudar, S.; van Duin, A.; Cheng, M.-J. *Top. Catal.* **2008**, *50*, 2.
(14) Nielson, K. D.; van Duin, A. C. T.; Oxgaard, J.; Deng, W. Q.; Goddard, W. A. *J. Phys. Chem. A* **2005**, *109*, 493.
(15) Chenoweth, K.; van Duin, A. C. T.; Dasgupta, S.; Goddard, W. A., III. *J. Phys. Chem. A* **2009**, *113*, 1740.
(16) Budzien, J.; Thompson, A. P.; Zybin, S. V. *J. Phys. Chem. B* **2009**, *113*, 13142.
(17) Liu, Y.; Goddard, W. A. *J. Phys. Chem. Lett.* **2010**, *1*, 2550.
(18) Rappe, A. K.; Casewit, C. J.; Colwell, K. S.; Goddard, W. A.; Skiff, W. M. *J. Am. Chem. Soc.* **1992**, *114*, 10024.
(19) Zhao, Y. X.; Spain, I. L. *Phys. Rev. B* **1989**, *40*, 993.
(20) Avitabile, G.; Napolitano, R.; Pirozzi, B.; Rouse, K.; Thomas, M.; Willis, B. *J. Polym. Sci.: Polym. Lett. Ed.* **1975**, *13*, 351.
(21) Keesom, W. H.; Köhler, J. W. L. *Physica* **1934**, *1*, 655.
(22) Wyckoff, R. *Crystal Structures*; Wiley: New York, 1963.
(23) Karasawa, N.; Dasgupta, S.; Goddard, W., III. *J. Phys. Chem.* **1991**, *95*, 2260.
(24) Barone, V.; Casarin, M.; Forrer, D.; Pavone, M.; Sambi, M.; Vittadini, A. *J. Comput. Chem.* **2009**, *30*, 934.
(25) Mortier, W. J.; Ghosh, S. K.; Shankar, S. *J. Am. Chem. Soc.* **1986**, *108*, 4315.
(26) Rappe, A. K.; Goddard, W. A. *J. Phys. Chem.* **1991**, *95*, 3358.
(27) Hanfland, M.; Beister, H.; Syassen, K. *Phys. Rev. B* **1989**, *39*, 12598.
(28) Ito, T.; Marui, H. *Polym. J.* **1971**, *2*, 768.
(29) Yoo, C.; Cynn, H.; Gygi, F.; Galli, G.; Iota, V.; Nicol, M.; Carlson, S.; Hausermann, D.; Mailhiot, C. *Phys. Rev. Lett.* **1999**, *83*, 5527.
(30) Aoki, K.; Yamawaki, H.; Sakashita, M.; Gotoh, Y.; Takemura, K. *Science* **1994**, *263*, 356.
(31) Davidson, A. J.; Oswald, I. D. H.; Francis, D. J.; Lennie, A. R.; Marshall, W. G.; Millar, D. I. A.; Pulham, C. R.; Warren, J. E.; Cumming, A. S. *CrystEngComm* **2008**, *10*, 162.
(32) Munday, L. B.; Chung, P. W.; Rice, B. M.; Solares, S. D. *J. Phys. Chem. B* **2011**, *115*, 4378.
(33) Smith, G. D.; Bharadwaj, R. K. *J. Phys. Chem. B* **1999**, *103*, 3570.
(34) Olinger, B.; Halleck, P.; Cady, H. *J. Chem. Phys.* **1975**, *62*, 4480.
(35) Stevens, L.; Velisavljevic, N.; Hooks, D.; Dattelbaum, D. *Propellants, Explos., Pyrotech.* **2008**, *33*, 286.
(36) Courtecuisse, S.; Cansell, F.; Fabre, D.; Petitet, J. P. *J. Chem. Phys.* **1995**, *102*, 968.
(37) Citroni, M.; Datchi, F.; Bini, R.; Di Vaira, M.; Pruzan, P.; Canny, B.; Schettino, V. *J. Phys. Chem. B* **2008**, *112*, 1095.
(38) Ouillon, R.; Pinan Lucarré, J. P.; Canny, B.; Pruzan, P.; Ranson, P. *J. Raman Spectrosc.* **2008**, *39*, 354.
(39) Zacharia, R.; Ulbricht, H.; Hertel, T. *Phys. Rev. B* **2004**, *69*, 155406.
(40) Billmeyer, F. W. *J. Appl. Phys.* **1957**, *28*, 1114.
(41) Usvyat, D.; Maschio, L.; Manby, F.; Casassa, S.; Schütz, M.; Pisani, C. *Phys. Rev. B* **2007**, *76*, 75102.
(42) Kjems, J. K.; Dolling, G. *Phys. Rev. B* **1975**, *11*, 1639.
(43) Cundall, R.; Palmer, T.; Wood, C. *J. Chem. Soc., Faraday Trans. 1* **1978**, *74*, 1339.
(44) Lau, K.; Hildenbrand, D.; Crouch-Baker, S.; Sanjurjo, A. *J. Chem. Eng. Data* **2004**, *49*, 544.
(45) Eiceman, G.; Preston, D.; Tiano, G.; Rodriguez, J.; Parmeter, J. *Talanta* **1997**, *45*, 57.
(46) Rosen, J.; Dickinson, C. *J. Chem. Eng. Data* **1969**, *14*, 120.
(47) Sorescu, D. C.; Rice, B. M.; Thompson, D. L. *J. Phys. Chem. B* **2000**, *104*, 8406.
(48) Olinger, B.; Roof, B.; Cady, H. *Proceeding of International Symposium on High Dynamic Pressures*; Commissariat a l'Energie Atomique: Paris, 1978; p 3.
(49) Peiris, S.; Gump, J. *Static Compression of Energetic Materials*; Springer: New York, 2008; p 99.